γ-Glutamyl Hydrolase: Kinetic Characterization of Isopeptide Hydrolysis Using Fluorogenic Substrates[†]

Jessica P. Alexander,[‡,§] Thomas J. Ryan,[||] David P. Ballou,[⊥] and James K. Coward*[,‡,#]

Departments of Chemistry, Medicinal Chemistry, and Biological Chemistry, The University of Michigan, Ann Arbor, Michigan 48109, and Laboratory of Molecular Diagnosis, Wadsworth Center, New York State Department of Health, Albany, New York 12201

Received August 9, 2007; Revised Manuscript Received November 28, 2007

ABSTRACT: γ-Glutamyl hydrolase, a cysteine peptidase, catalyzes the hydrolysis of poly-γ-glutamate derivatives of folate cofactors and many antifolate drugs. We have used internally quenched fluorogenic derivatives of glutamyl-γ-glutamate and (4,4-difluoro)glutamyl-γ-glutamate to examine the effect of fluorine substitution adjacent to the scissile isopeptide bond. Using a newly developed continuous fluorescence assay, the hydrolysis of both substrates could be described by Michaelis–Menten kinetics. Fluorine substitution resulted in a significant decrease in observed rates of hydrolysis under steady-state conditions due primarily to a ∼15-fold increase in K_m. Using stopped-flow techniques, hydrolysis of the non-fluorinated isopeptide was characterized by a burst phase followed by a steady-state rate, indicating that formation of the acyl enzyme is not rate-limiting for hydrolysis of this isopeptide. This conclusion was confirmed by analysis of the progress curves over a wide range of substrate concentration, which demonstrated that the acylation rate (k_2) is ∼10-fold higher than the deacylation rate (k_3). The increased value of K_m associated with the difluoro derivative limited the ability to obtain comparable pre-steady-state kinetics data at saturating concentration of substrate due to inner filter effects. However, even under nonsaturating conditions, a modest burst was observed for the difluoro derivative. These data indicate that either deacylation or rearrangement of the enzyme–product complex is rate-limiting in this isopeptide hydrolysis reaction.

γ-Glutamyl hydrolase (GH,[1] EC 3.4.19.9), a lysosomal cysteine protease, plays an important role in maintaining folate homeostasis (*1*). The folates are key cofactors in one-carbon metabolism leading to such essential biosynthetic products as glycine, methionine, thymidylate, and purine nucleotides (*2*, *3*). The folylmonoglutamates are elongated to folylpolyglutamates by the enzyme folylpoly-γ-glutamate synthetase (FPGS, EC 6.3.2.17) in an ATP-dependent ligation process, effectively trapping the cofactor in the cell (*4*, *5*). GH catalyzes the hydrolysis of the Glu-γ-Glu bonds to form folylmonoglutamates that can then be exported from the cell. Thus, these two enzymes are primarily responsible for the regulation of folate levels in the cell (Figure 1).

Consistent with this notion, high GH activity has also been shown to decrease the efficacy of several polyglutamylated antifolate chemotherapeutic drugs such as methotrexate (AMPte-Glu) (*1*). The polyglutamylated drug is hydrolyzed by GH, generating "free" drug that is retained poorly and leads to reduced cytotoxicity. A number of single nucleotide polymorphisms (SNPs) have been identified in the human GH gene both in the promoter region and the mature enzyme (*6*). One of these SNPs has been found in acute lymphoblastic leukemia patients with low GH activity. This SNP has been shown to reduce GH activity on long-chain methotrexate polyglutamates leading to the accumulation of intracellular methotrexate polyglutamates in leukemia cells (*7*). These reports place GH as an integral component in the regulation of the intracellular level of both folates and multiple antifolate drugs.

We have developed fluoroglutamate-containing γ-glutamyl peptides as mechanistic probes for GH (*8*). In earlier studies

* Author to whom correspondence should be addressed. University of Michigan, 3813 Chemistry, 930 N. University, Ann Arbor, MI 48109-1055. Phone: 734-936-2843. Fax: 734-647-4865. E-mail: jkcoward@umich.edu.

‡ Department of Chemistry, University of Michigan.

§ Present address: Department of Infectious Disease, Merck & Co., Rahway, NJ 07065.

|| Laboratory of Molecular Diagnosis, Wadsworth Center, New York State Department of Health.

⊥ Department of Biological Chemistry, University of Michigan Medical School.

Department of Medicinal Chemistry, University of Michigan.

[1] Abbreviations: Abz, *o*-aminobenzoyl; AMPteGlu, 2-deoxy-2-amino-10-methyl-pteroyl; (2′RS,4′RS), indicates racemic carbon at the 2′- and 4′-positions; AMPte-(4-FGlu), 2-deoxy-2-amino-10-methyl-pteroyl(4-fluoro)glutamic acid; BME, β-mercaptoethanol; DIPEA, diisopropylethylamine; DMAP, dimethylaminopyridine; DMF, dimethylformamide; EDC, *N*-(3-dimethylaminopropyl)-*N*′-ethylcarbodiimide; EDTA, ethylenediaminetetraacetic acid; EtN₃, triethylamine; Fmoc, fluorenylmethyloxycarbonyl; FRET, fluorescence resonance energy transfer; GH, γ-glutamyl hydrolase; HETCOR, heteronuclear correlation spectroscopy; HBTU, *N,N,N′,N′*-tetramethyl-*O*-(1*H*-benzotriazol-1-yl)-uronium hexafluorophosphate; HOBt, 1-hydroxybenzotriazole; IFE, inner filter effect; *N*-Me-*p*AB, *N*-methyl-*p*-aminobenzoyl; SPPS, solid phase peptide synthesis; TCEP, tris(2-carboxyethyl)phosphine hydrochloride; TEAB, triethylammonium bicarbonate; TFA, trifluoroacetic acid; Tyr(NO₂), 3-nitrotyrosine.
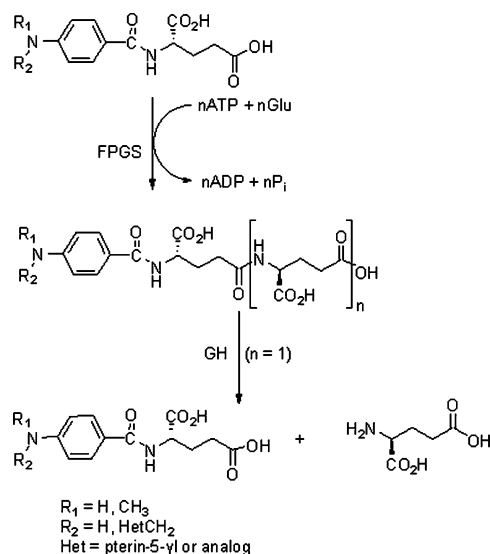
FIGURE 1: Folylpolyglutamate synthesis and hydrolysis. The folylmonoglutamate is elongated in an ATP-dependent reaction catalyzed by FPGS. GH catalyzes the hydrolysis of the γ-glutamyl bonds.

with GH from hog kidney, it was observed that a methotrexate derivative, 2-amino-10-methylpteroyl ($2'RS$,$4'RS$)-4-fluoroglutamyl-γ-glutamate (AMPte-(4-F)Glu-γ-Glu), was hydrolyzed significantly more slowly than AMPte-Glu-γ-Glu (*9*). These findings were corroborated with recombinant rat and human enzymes where it was found that substrates containing either (2S,4S)-4-fluoroglutamate (*10*) or (2RS)-4,4-difluoroglutamate (*11*) were hydrolyzed at least 25-fold more slowly than their non-fluorinated analogues (*12*). Fluorine substitution for hydrogen is sterically conservative but imparts large electronic effects that can change rates of reaction (*13*). It was of interest to determine the mechanistic basis for the attenuated rate of GH-catalyzed hydrolysis of the fluoroglutamate-containing substrates. In the studies reported here, recombinantly expressed rat GH was used, as it not only has demonstrated greater activity on shorter peptides than human GH, but also exhibits an apparent endopeptidase mode of cleavage that results in products that are not further substrates for the enzyme (*14*, *15*), thereby simplifying the kinetics analysis.

Despite the interest in GH, protocols available for measuring its activity have been limited to end-point assays of cleavage products using high-performance liquid chromatography (*16−20*) or capillary electrophoresis (*21*, *22*). We have reported the first continuous assay for GH based on an internally quenched fluorogenic glutamyl-γ-glutamyl peptide with an N-terminal N-methyl-p-aminobenzoyl (N-Me-pAB) moiety as the fluorophore (*23*). Its fluorescence is quenched in the intact substrate by fluorescence resonance energy transfer (FRET) (*24*) to a C-terminal 3-nitrotyrosine (Tyr-(NO$_2$)). Cleavage of the Glu-γ-Glu bond results in release of the Tyr(NO$_2$) moiety, so that fluorescence of the N-terminal hydrolysis product is observed. However, this substrate could only be used at concentrations up to about 10 μM because the strong absorbance of the N-Me-pAB moiety results in a decrease in the observed fluorescence at higher substrate concentrations, a phenomenon commonly referred to as the inner filter effect (IFE) (*24*). A second-generation fluorogenic substrate (**1**, Figure 2), in which the N-Me-pAB fluorophore is replaced with an o-aminobenzoyl
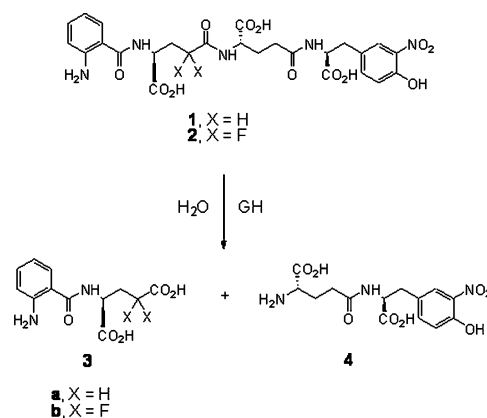

FIGURE 2: GH-catalyzed hydrolysis of internally quenched fluorescent substrates **1** and **2**.

(Abz) group, extends the useful concentration range before significant inner filter effects are observed and provides better sensitivity with a larger fluorescent signal. In order to study directly the influence of fluorine on GH-catalyzed hydrolysis of γ-glutamyl peptides, 4,4-difluoroglutamate has also been incorporated into this framework (**2**, Figure 2) (*25*). These compounds have been used in a continuous fluorescence assay to provide a detailed kinetic comparison between the GH-catalyzed hydrolysis of glutamyl and fluoroglutamyl peptide substrates. The studies described herein define the steady-state kinetic parameters for GH-catalyzed hydrolysis of **1** and **2**. Transient kinetic parameters were determined using stopped-flow fluorescence spectroscopy. These experiments provide the first definitive evidence for formation of an intermediate in the reaction catalyzed by GH. Based on the steady-state and transient kinetics data, possible mechanisms for fluorine-mediated modulation of γ-glutamyl peptide hydrolysis are discussed.

EXPERIMENTAL PROCEDURES

Materials, general synthetic methods, and details on the solution phase synthesis of **1** (Scheme 1) are described in the Supporting Information, as is the expression and purification of rat GH. The syntheses of N-Abz-Glu·TFA (**3a**) and Glu-γ-Tyr(NO$_2$)·Et$_3$N (**4**), the two expected products resulting from GH-catalyzed hydrolysis of **1** (Figure 2), are also described in the Supporting Information. For access to larger amounts of **1** required for transient kinetics experiments, isopeptide **1** was also synthesized by manual solid phase peptide synthesis on Wang resin (1.00 g, 1.2 mmol, suspended in 10 mL dry DMF) using an Fmoc protection scheme and HBTU activation (Scheme 2, see Supporting Information for details). Abz-4,4-F$_2$Glu-γ-Glu-γ-Tyr(NO$_2$) (**2**) was synthesized by Dr. David Konas (*25*).

Analytical HPLC was controlled and monitored using either two Altex pumps, a Hewlett-Packard diode array UV/vis detector and an HP workstation, or a Waters system with a 6000a pump and a 510 pump with a Waters 996 photodiode array detector running under Millenium[32] software (version 3.2). A Vydac 218TP54 C$_{18}$ analytical column was eluted at 1 mL/min under one of the following conditions. Solvents: A, acetonitrile with 0.1% AcOH and 0.02% TFA (v/v); B, H$_2$O with 0.1% AcOH and 0.02% TFA (v/v). Gradient 1: a separation beginning with 15% solvent A and 85% solvent B, which increased to 20% A over 25 min, then

Scheme 1
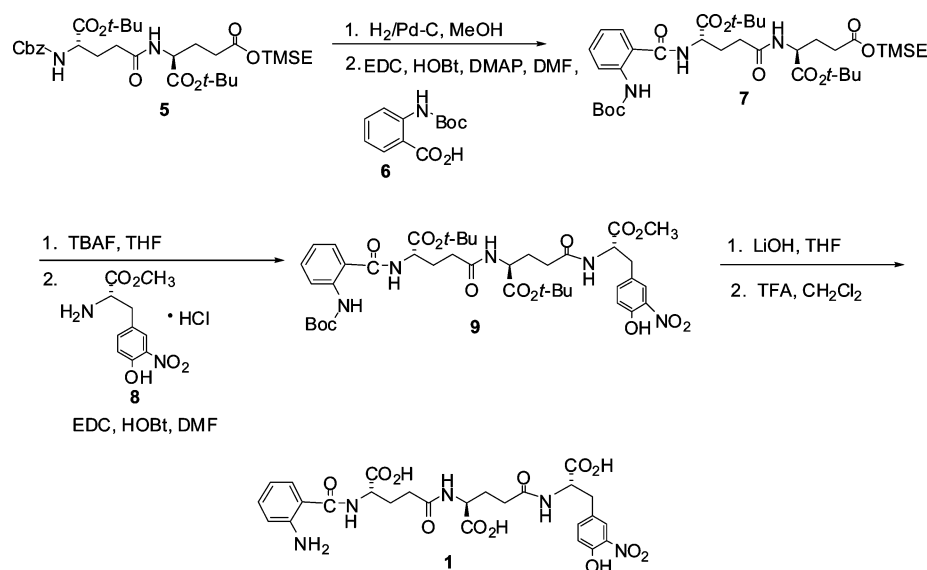
Scheme 2
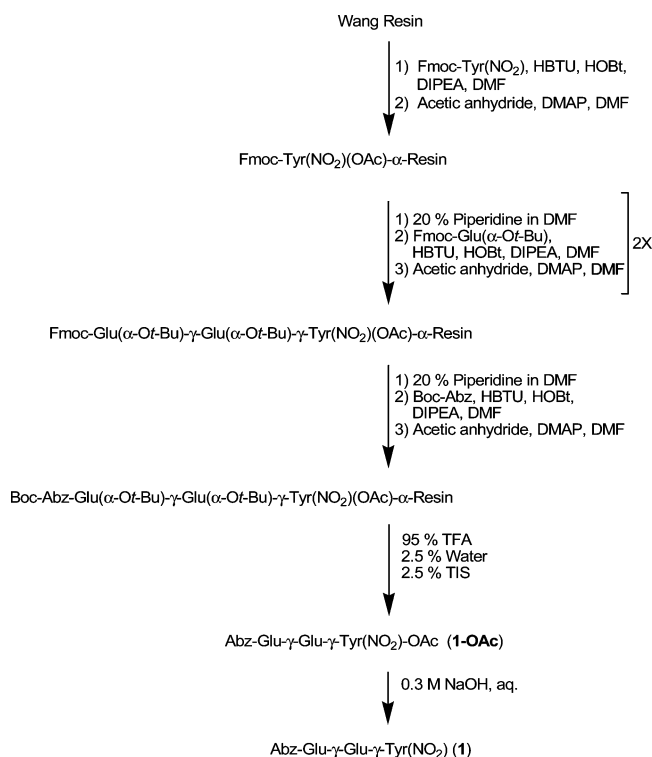
ramped to 95% solvent A in 15 min. Gradient 2: a separation beginning with 3% solvent A and 97% solvent B, which was linearly increased to 50% A over 43 min, and then ramped to 95% solvent A in 2 min.

LC−MS analysis was performed on a system including a Finnigan LCQ mass spectrometer interfaced with either a Hitachi HPLC and Hitachi detector (UV or fluorescence), or ThermoFinnigan Surveyor HPLC components with a fluorescence detector incorporated into the system using a splitter between the fluorescence detector and mass spectrometer. The HPLC separation was conducted on a Vydac C_{18} column with a gradient elution of solvent A and solvent B with either (gradient 3) a linear increase from 3% to 50% solvent A over 22 min at 1 mL/min or (gradient 4) a linear increase from 3% solvent A to 50% solvent B over 43 min

at 0.8 mL/min. UV detection was set at 230 and 278 nm, and fluorescence detection was set at $\lambda_{ex} = 320$ nm, $\lambda_{em} = 420$ nm for Abz-containing compounds.

Initial Biochemical Characterization of FRET Peptides. Abz-Glu-γ-Glu-γ-Tyr(NO$_2$) Enzymatic Hydrolysis: LC−MS Analysis. Abz-Glu-γ-Glu-γ-Tyr(NO$_2$) (**1**, 50 μM) was incubated with GH (0.72 nM) for 85 min. The resulting mixture was analyzed by LC−MS (Hitachi HPLC components, gradient 3); $t_R = 8.0$ min, $(M + H)^+$ m/z 266.9 (**3a**); $t_R = 9.0$ min, $(M + H)^+$ m/z 356.1 (**4**).

Extinction Coefficient of Abz-Glu-γ-Glu-γ-Tyr(NO$_2$) (1). Insufficient quantities of **1** and **2** were available by solution phase synthesis for accurate determination of an extinction coefficient for these substrates. Therefore, the extinction coefficients of the N-terminal chromophore, N-Abz-glutamic acid, **3a**, and the C-terminal chromophore, N-Ac-3-nitrotyrosine, **S3**, were obtained to provide an accurate extinction coefficient for the intact peptides. *N*-Acetyl-3-nitrotyrosine (**S3**, Supporting Information, 268.2 mg, 1.0 mmol), previously dried over P$_2$O$_5$ at 25 °C for 12 h, was dissolved in 2 L of Milli-Q water to provide a 500 μM stock solution. Similarly, Abz-Glu (**3a**, Supporting Information, 132.9 mg, 0.5 mmol), previously dried over P$_2$O$_5$ at 25 °C for 12 h, was weighed under N$_2$. This was diluted to 1 L in H$_2$O to provide a 500 μM stock solution. These stock solutions were diluted in either 0.1 M HCl or 0.1 M NaOH to provide 1 mL volumes with final concentrations of 2, 5, 10, 25, 50, 75, and 100 μM. All dilutions were made in triplicate. Spectra were recorded between 220 and 600 nm at a scan rate of 600 nm/min at each concentration in each solvent. Plots of the average absorbance at 278.5 nm (0.1 M HCl) or 285 nm (0.1 M NaOH) versus concentration were then fit to Beer's law and the extinction coefficients of each chromophore summed to give values of $\epsilon = 6690$ M^{-1} cm^{-1} ($\lambda = 278.5$ nm, 0.1 M HCl) and $\epsilon = 5080$ M^{-1} cm^{-1} ($\lambda = 285$ nm, 0.1 M NaOH).[2] Following successful synthesis of **1** on a larger scale by solid phase synthesis, direct determination of the

---

[2] Determination of the extinction coefficient for **S3** (2-100 μM) in 0.2 M Tris-0.2 M NaCl, pH 10, gave a value of $\epsilon = 4380$ M^{-1} cm^{-1}, in agreement with that reported in the literature under identical conditions (60).

extinction coefficient was possible and led to a value of $\epsilon = 5110$ M^{-1} cm^{-1} ($\lambda = 285$ nm, 0.1 M NaOH), in good agreement with that determined for **1** as described above. Considering the identical chromophores in the donor and acceptor moieties of **1** and **2**, the extinction coefficient of **2** was assumed to be the same as that determined for **1**.[3]

Enzyme Assays. Protein Concentration. For routine determination of protein concentration, the method of Bradford (*26*) was used with reagents purchased from either BioRad or Sigma. The manufacturer's instructions for the microassay were followed, and bovine serum albumin was used as the standard. Initially, for steady-state experiments, the GH concentration was determined by the Bradford assay adjusted for enzyme purity (ca 75%) based on quantitative SDS–PAGE gel analysis. A more reliable determination of active GH concentration using highly purified GH was obtained by a further adjustment based on a fit to the pre-steady-state kinetics data (eq 1–3); *vide infra*. Concentrations of GH determined in this manner are indicated in all stopped-flow experimental protocols and were used in the calculation of rate constants (Table 1, entries 2 and 4).

Continuous Steady-State Kinetic Analysis. Concentrations of stock solutions of Abz-Glu-γ-Glu-γ-Tyr(NO$_2$) were determined based on the UV absorbance at 285 nm ($\epsilon = 5080$ M^{-1} cm^{-1}, *vide supra*) in 0.1 M NaOH. All solutions except those of the enzyme were passed through a 0.2 μm syringe filter or a spin filter. In a typical assay, 90 μL of assay buffer pH 6.0, containing 50 mM β-mercaptoethanol, 50 mM sodium acetate, and **1** or **2** (concentration varied), was equilibrated at 25 °C in an amber microcentrifuge tube. The stock solution of GH was centrifuged at 10,000 rpm (8000*g*) for 2 min to sediment any dust particles, and the supernatant was then carefully removed and diluted 10-fold in storage buffer consisting of 50 mM sodium acetate pH 5.5, 50 mM BME, 1 mM octyl-β-glucopyranoside, 1 mM EDTA, 1 M NaCl, pH 5.5. Preincubation of GH (15 μL) at 25 °C for 2 h was necessary to obtain maximal GH activity that appeared to be stable for at least the next 6 h (*14*). To initiate the reaction, an aliquot of activated GH (10 μL) was added to the assay buffer and substrate in a microcuvette positioned in a jacketed cell holder. Final concentrations were typically 50 mM sodium acetate, pH 6.0, 50 mM BME, 0.25–75 μM substrate (**1** or **2**), and 0.72 nM GH (**1**) or 6.4 nM GH (**2**) in a final volume of 100 μL.

Reaction progress was monitored by time-based fluorescence acquisition (Spex Fluoromax-2) with the following parameters: time interval 1 s, integration 1.0 s, slit width 5 nm (band-pass), $\lambda_{ex} = 320$ nm, $\lambda_{em} = 420$ nm. The cuvette was capped tightly, and the fluorescence was monitored for 2–10 min. Samples were transferred from the microcuvette to amber microcentrifuge tubes, and a 1 μL aliquot of concentrated GH (typically 2.9 μM final concentration) was added to hydrolyze completely the remaining substrate. The controls at each concentration of substrate were treated as above except that GH storage buffer was added in place of GH. Both sample and control tubes were incubated at 25 °C

to allow complete hydrolysis of the samples, and the final fluorescence was measured for 25 s with an interval of 5 s and integration time of 1 s to provide the fluorescence end points (F_∞).

The corrected fluorescence was obtained by subtracting the fluorescence of the control from that of the corresponding sample. Samples with substrate concentrations >20 μM were corrected for IFE (*vide infra*). A calibration curve to convert fluorescence units to micromolar product was created by plotting IFE-corrected F_∞ vs substrate concentration. The inverse of the slope of this line (μM/fluorescence unit) multiplied by the initial rate in fluorescence units/s provides the initial rate in units of μM/s. Initial rates were then fit to the Michaelis–Menten equation. To determine k_{cat}, V_{max} was divided by the total enzyme concentration. Data fitting was completed in Kaleidagraph version 3.5 (Synergy software, Reading, PA).

Inner Filter Effect Corrections. Solutions containing varying concentrations (0.25–75 μM) of equimolar Abz-Glu and Glu-γ-Tyr(NO$_2$) were used to determine a correction factor for each concentration of substrate used in the assay. The measured fluorescence divided by the correction factor provided the corrected fluorescence value. This IFE correction was applied to initial rates measured at the higher substrate concentrations of **1** or **2** (35, 50, and 75 μM), whereby the initial rate was divided by an appropriate correction factor (0.91, 0.90, or 0.62 respectively). Final fluorescence values obtained by hydrolysis of **1** or **2** (10, 20, 35, 50, and 75 μM) were similarly corrected (factors of 0.97, 0.92, 0.83, 0.77, and 0.55 respectively).

Transient Kinetics. Transient kinetics experiments were carried out on Hi-Tech SF-61 or Hi-Tech SF-61DX2 stopped-flow instruments with a xenon lamp as the light source. The excitation wavelength was 320 nm (unless otherwise noted), and a 389 nm cutoff filter was used to select the emission wavelengths. Experiments were initiated by mixing equal volumes of enzyme and substrate at 25 °C or 4 °C. The substrate solutions were prepared in 50 mM sodium acetate, pH 6.0, 50 mM BME. Substrate concentrations are reported as final concentration after mixing with GH. Unless otherwise noted, solutions of GH were prepared in GH storage buffer, pH 5.5 with [NaCl] = 0.2 M to obtain a final concentration 0.1 M [NaCl] after mixing with substrate. Data were collected to at least 10 s using the program KISS (Kinetic Instruments, Inc., Ann Arbor, MI) on the Hi-Tech single-mixing stopped-flow instrument or KinetAsyst on the SF-61DX2. The dead time of the instrument is 1.5–2 ms. Data were collected at least in triplicate unless otherwise noted and were corrected by subtracting the fluorescence of the intact substrate. Standard curves were generated by measuring the fluorescence of solutions of various concentrations of the fluorescent hydrolysis product, Abz-Glu, varying concentrations of a 1:1 mixture of the reaction products, Abz-Glu and Glu-Tyr(NO$_2$) or *N*-Acetyl-Tyr(NO$_2$), or by internal calibration based on end points of completely hydrolyzed samples.

For samples exhibiting a burst phase, the average progress curves out to 0.5 s were fit to the burst equation (eq 1)

$$P = A(1 - e^{-kt}) + vt + C \qquad (1)$$

where *P* represents the product formed in terms of fluores-

---

[3] In the synthesis of **2** (*25*), a different synthetic route was used to access a fully protected intermediate corresponding to **9** (Scheme 1). Therefore, the *N*-terminal chromophore, *N*-Abz-(4,4-difluoro)glutamic acid, corresponding to **3a** was not available for use in determining the extinction coefficient of **2**.

cence, A is the amplitude of the burst, k is the burst rate (k_{burst}), t is the time in seconds after mixing, v is the slope of the steady-state linear part of the curve (v_{ss}), and C is the intercept extrapolated from the linear portion (*27, 28*). In experiments varying $[S]_0$ at constant $[GH]$, the progress curves were fit to obtain k_{burst}. A plot of k_{burst} versus substrate concentration was fit to eq 2 (*27, 28*). A plot of the burst amplitude (A in eq 1) versus substrate concentration was fit to eq 3 (*27, 28*). $[E]$ is known from the stoichiometry of the

$$k_{burst} = (k_2 + k_3)[S]/(K_s + [S]) \qquad (2)$$

$$A = [E](k_2/(k_2 + k_3))^2/(1 + (K_m/[S]))^2 \qquad (3)$$

burst, and K_m is known from fitting the Michaelis−Menten equation, using v_{ss} (from eq 1) as the steady-state rate. Thus, a fit of the data to eq 2 provides a value of $(k_2 + k_3)$ as well as K_s. Using the value of $(k_2 + k_3)$ thus obtained, a fit of eq 3 provides a value of k_2. Subtraction of k_2 from $(k_2 + k_3)$ provides the value for k_3.

RESULTS

Synthesis of FRET Peptide Substrate for GH. A γ-glutamyl peptide with the *o*-aminobenzoyl fluorophore at the *N*-terminus and the 3-nitrotyrosine quenching moiety at the *C*-terminus was first synthesized as shown in Scheme 1 (see Supporting Information for details). Compound **5**, a protected diglutamyl peptide (*23*),[4] was deprotected at the *N*-terminus and coupled to Boc-protected *o*-aminobenzoic acid (**6**) using standard EDC-mediated peptide coupling. This was followed by deprotection of the *C*-terminus, coupling of the 3-nitro-tyrosine quenching moiety (**8**), and two deprotection steps to provide the desired product, **1**. To study directly the effect of fluorine on GH-catalyzed hydrolysis of γ-glutamyl pep-tides, 4,4-difluoroglutamate was also incorporated using the same synthetic strategy to provide the related fluoropeptide, **2** (*25*). The two putative products of GH-catalyzed hydrolysis of **1**, Abz-Glu (**3a**) and Glu-Tyr(NO$_2$) (**4**) (Figure 2), were also synthesized for use as HPLC standards, LC−MS standards, and for fluorescence standard curves (see Sup-porting Information for details).

For transient kinetic studies, an additional supply of **1** was obtained using solid phase peptide synthesis (SPPS) to provide ample quantities of **1** in a rapid, efficient synthesis (Scheme 2). As described in the Supporting Information, SPPS is the preferred method of preparing **1**, due to the commercial availability of suitably protected natural amino acids. However, SPPS is currently not yet feasible for synthesis of **2** or other peptides containing non-natural amino acids due to the large excess of Fmoc-protected amino acid (e.g., (2*S*)-4,4-difluoroglutamic acid) required for coupling to the resin-based *C*-terminus of the growing peptide.

Enzyme Assay Development for GH. To facilitate detailed kinetic studies of GH-catalyzed hydrolysis of both non-fluorinated and fluorinated substrates, our recently reported FRET assay for GH has been further refined. The original assay was based on an internally quenched fluorogenic glutamyl-γ-glutamyl peptide with an *N*-terminal *N*-methyl-

p-aminobenzoyl (*N*-Me-*p*AB) moiety as the fluorophore and 3-nitrotyrosine as the *C*-terminal quenching moiety (*23*). However, the *N*-Me-*p*AB moiety has a significant absorbance ($\lambda_{max} = 289$ nm, $\epsilon = 15,050$ M^{-1} cm^{-1}, 0.1 N NaOH (*29*)) near the excitation wavelength ($\lambda_{ex} = 290$), leading to a large IFE that limits the use of this substrate to concentrations below 10 μM. In the second-generation fluorogenic substrate (**1**), the *N*-Me-*p*-AB fluorophore has been replaced with an *o*-aminobenzoyl (Abz) group $\lambda_{max} = 322$ nm, $\epsilon = 1,585$ M^{-1} cm^{-1}, ethanol (*30*)) so that absorbance is much less at the excitation wavelength ($\lambda_{ex} = 320$ nm). The use of **1** extends the concentration range (0−35 μM) before significant inner filter effects are observed as well as provides better sensitivity with a higher fluorescent signal. The concentration range of **1** and **2** in assays could be further extended to 75 μM by correcting for the IFE as described in Experimental Proce-dures. A more rigorous method of calibrating the assay to convert the fluorescence units to micromolar product also improved the reproducibility of the assay. Instead of using a single calibration point as is frequently reported for FRET assays, a concentrated aliquot of GH (1 μL, 2.9 μM) was added to each assay (varying concentrations of **1** or **2**) after the initial velocity measurement, and the fluorescence was measured after complete hydrolysis. A linear plot of fluo-rescence versus product concentration (see Supporting Information, Figure S1) provided a reliable calibration factor as the inverse slope of the line (μM/fluorescence units). These improvements resulted in a robust, sensitive, and convenient continuous assay for GH that could now be applied to the detailed kinetic analysis of **1** and **2**.

Steady-State Kinetic Comparison of GH-Catalyzed Hy-drolysis of Substrates 1 and 2. The steady-state kinetic parameters for GH reactions with **1** and **2** were determined at 25 °C using the fluorescence assay (see Supporting Information, Figure S2). Since the rate of hydrolysis of **2** is significantly slower than that of **1** (*vide infra*), a higher concentration of GH ($\sim$9-fold) was used to monitor the reaction of **2** (see Experimental Procedures). The kinetics data were fit to the Michaelis−Menten equation to provide values of K_m and V_{max} for **1** and **2**, which are summarized in Table S1. Because it was necessary to use a higher concentration of GH in order to obtain reasonable rates of hydrolysis of **2**, a comparison of k_{cat} and k_{cat}/K_m for the two substrates is more appropriate than V_{max} and K_m. However, given the observation of an attenuated burst amplitude in the GH-catalyzed hydrolysis of **1** under pre-steady-state conditions ($[S] \approx [GH]$, *vide infra*), determination of k_{cat} under steady-state conditions by this method should be done with caution in this case. With these caveats, the substrate specificity of GH, as indicated by the *relative* values of k_{cat}/K_m, showed a 25-fold preference for **1** over **2**. These data are consistent with preliminary data obtained with several isopeptide derivatives of methotrexate, 2-amino-10-meth-ylpteroyl (2*RS*,4*RS*)-4-fluoroglutamyl-γ-glutamate (AMPte-(4-F)Glu-γ-Glu) (*9*), and the corresponding derivatives containing either (2*S*,4*S*)-4-fluoroglutamate or (2*RS*)-4,4-fluoroglutamate (*12*). This difference appears to be mediated mainly by a much higher value of K_m (75 μM) for the fluorinated analogue, **2**, over that of **1** ($K_m = 5.4$ μM). The high value of K_m for **2** made it difficult to saturate GH before inner filter effects became too severe, leading to slightly

---

[4] Although intermediate **5** was reported previously (*23*), details on its synthesis were not provided. These details are included herein (see Supporting Information).

$$E + S \underset{k_{-1}}{\overset{k_1}{\rightleftharpoons}} ES \underset{k_{-2}}{\overset{k_2}{\rightleftharpoons}} ES' \overset{k_3}{\longrightarrow} E$$

$$P_1 = (Glu\text{-}\gamma\text{-}Tyr(NO_2))$$

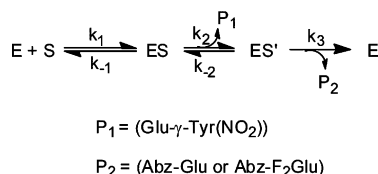$$P_2 = (Abz\text{-}Glu \text{ or } Abz\text{-}F_2Glu)$$

FIGURE 3: Proposed kinetic scheme for GH. ES is the Michaelis complex, and ES′ is the acyl enzyme.

higher errors in the determination of the kinetic constants for **2** compared to **1**.

The proposed kinetic scheme for GH, that of a typical protease, is shown in Figure 3. In this scheme, rapid equilibrium association of the enzyme and substrate forms the Michaelis complex (ES), followed by formation of the acyl enzyme (ES′) with concomitant release of the first product P_1 (Glu-Tyr(NO₂) (**4**)). Separation of the quenching moiety (Tyr(NO₂)) from the fluorophore (Abz) in this step results in increased fluorescence because FRET is distance-dependent. The last step of the kinetic scheme is the hydrolysis of the acyl−enzyme intermediate to release the second product, P_2 (Abz-Glu (**3a**) or Abz-F₂Glu (**3b**)). Both the formation of the acyl enzyme and the hydrolysis of the acyl enzyme (to re-form free enzyme) proceed through similar tetrahedral intermediates (*31*). The slower hydrolysis of the fluorinated analogue, **2**, could be due either to steric effects that result in poor binding to GH or to an electronic effect, perhaps involving the stabilization of one or both tetrahedral intermediates by adjacent fluorine substituents (*32*).

Steady-State vs Pre-Steady-State Kinetics Experiments. From the above steady-state kinetics data alone it is difficult to draw conclusions about the mechanistic differences in the hydrolysis of **1** compared to **2**. The values of K_m for **1** and **2** as determined under steady-state conditions differ by almost 15-fold. K_m is defined by the individual rate constants shown in eq 4 and is not equivalent to the dissociation constant

$$K_m = (k_{-1}/k_1)[k_3/(k_2 + k_3)] \quad (4)$$

($K_s = k_{-1}/k_1$) unless acylation is rate-limiting; i.e., $k_2 \ll k_3$, and $k_{-1} \gg k_2$. Pre-steady-state kinetics experiments can often allow for deconvolution of K_m to provide individual rate constants. These experiments should therefore allow for independent determination of k_{cat} under conditions where [GH] is identical for experiments involving isopeptides, **1** and **2**. In the mechanism shown in Figure 3, k_{cat} is defined by eq 5. The value of k_{cat} provides a lower limit for the first-

$$k_{cat} = k_2 k_3/(k_2 + k_3) \quad (5)$$

order rate constant governing all steps, including chemical and conformational changes, in converting substrate to product once the substrate is bound to the enzyme surface (*28*). It is assumed that k_{-2} approaches zero due to the low concentration of P_1 as it diffuses away from the protein, leading to decreased FRET and increased fluorescence. Stopped-flow kinetic experiments were conducted to determine if k_3 might be the rate-limiting step.

*Pre-Steady-State Kinetics Experiments for GH and **1**.* Varying concentrations of GH were mixed with 50 μM **1** (~10× K_m) in the stopped-flow instrument, and the increase in fluorescence was monitored continuously. The results at
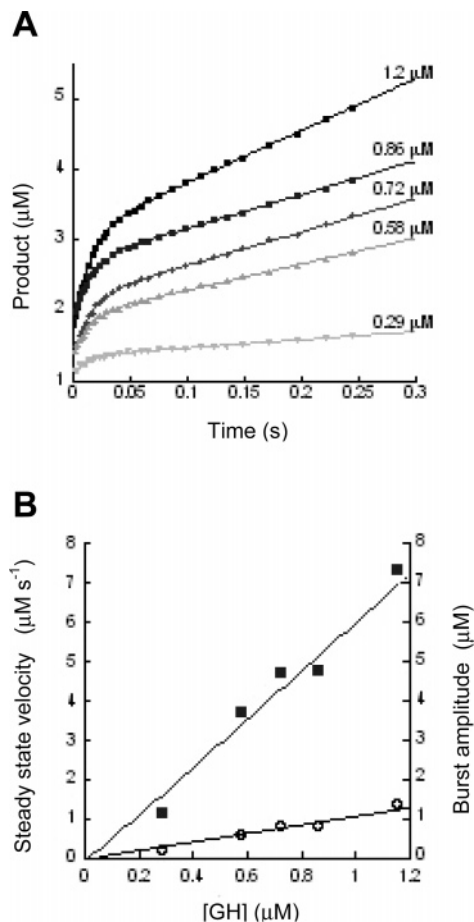
FIGURE 4: (A) Burst observed for rapid mixing of Abz-Glu-γ-Glu-γ-Tyr(NO₂) (**1**, 50 μM) in assay buffer, pH 6.0, and varying concentrations of GH, in enzyme storage buffer, pH 5.5, 4 °C. Final concentrations were 50 μM **1** and 0.29−1.2 μM GH as indicated. Each progress curve is the average of five experimental traces. Only 10% of the data points are shown for clarity, and each line represents a fit to the burst equation (eq 1). (B) Dependence of the burst amplitude (○) and steady-state velocity (■) on enzyme concentration.

25 °C suggested the presence of a burst; however, lowering the temperature to 4 °C allowed the observation of a significant burst (Figure 4A). The burst suggests formation of an intermediate on the reaction pathway, the breakdown or release of which is slow relative to the rate of production of the first observed product. The observed burst curve indicates that k_3, representing hydrolysis of the acyl enzyme intermediate and release of Abz-Glu, is the rate-limiting step of the reaction.[5] Fitting progress curves to the burst equation (eq 1) provided a rate constant for the initial phase of 72 s⁻¹, independent of [GH] (Figure 4A, [**1**] = 50 μM, ca. 10K_m). The amplitude of the burst and the steady-state rate, v_{ss}, at each concentration of enzyme (Figure 4A) were determined and shown to be proportional to the enzyme concentration (Figure 4B). Assuming a full burst, the burst amplitude provides an estimate of the viable active site concentration. However, this was determined to be only about 30% of the GH concentration indicated by Bradford assay (data not shown). Several possible factors that could result in attenuation of the burst amplitude are discussed below.

---

[5] The rate constant, k_3, may of course represent more than one step in the reaction pathway.
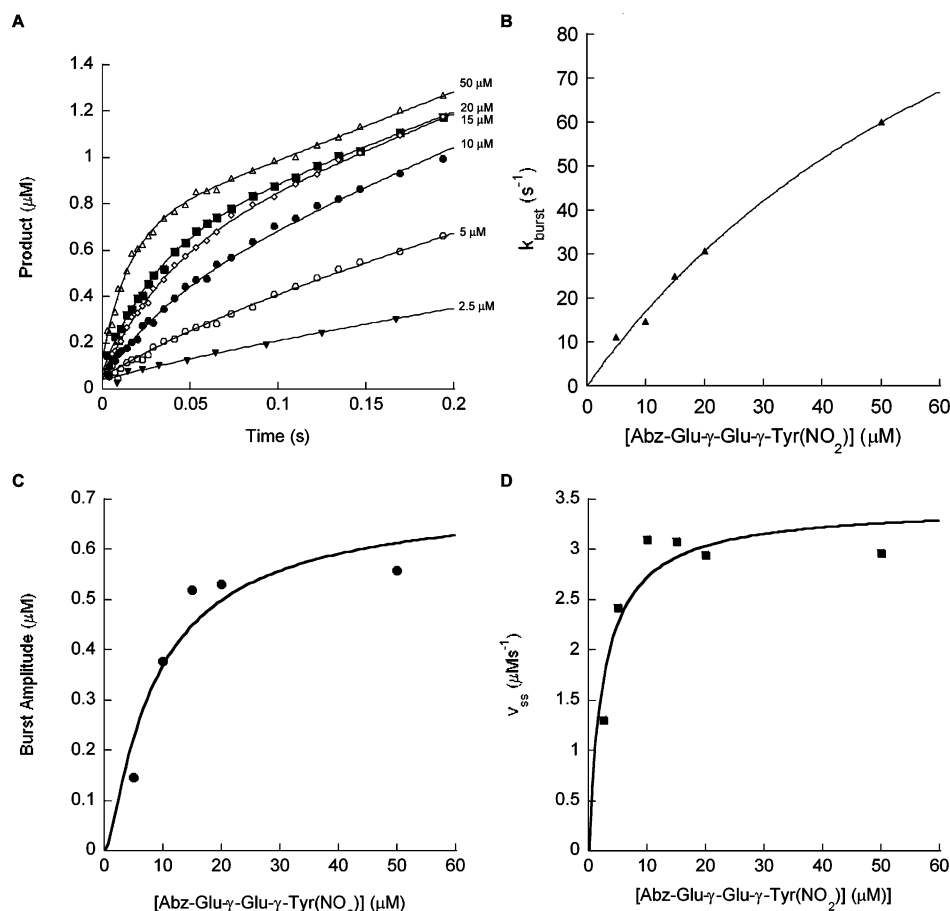
FIGURE 5: Transient kinetics with varying Abz-Glu-γ-Glu-γ-Tyr(NO$_2$), **1**, in assay buffer, pH 6.0, mixed with GH (0.86 μM final concentration after mixing), in enzyme storage buffer, pH 5.5, 4 °C. (A) Burst kinetics observed by fluorescence at >389 nm upon varying concentration of **1** (indicated on figure). Each progress curve is the average of at least three experimental traces, and only 10% of the data are shown for clarity. Data for [**1**] > 2.5 μM were fit to eq 1 (solid lines). Data for **1** > 2.5 μM were fit to eq 1. (B) Dependence of burst rate constant on substrate concentration with fit to eq 2. (C) Dependence of burst amplitude on substrate concentration with fit to eq 3. (D) Dependence of steady-state rate on substrate concentration with fit to the Michaelis−Menten equation.

At a fixed concentration of GH (0.86 μM), the kinetics of hydrolysis of **1** (2.5−50 μM) were monitored by fluorescence and fit to eq 1 (Figure 5A) to obtain the burst rate constants (k) and amplitudes (A), as well as the steady-state velocities (v_{ss}). At concentrations of **1** less than K_m (e.g., 2.5 μM), a burst was not observed at the concentration of GH used, so this progress curve was only used for fitting the steady-state velocity. This dependence of the burst rate constant on substrate concentration was fit to eq 2 (Figure 5B), which provides values for K_s and ($k_2 + k_3$), and the dependence of the burst amplitude on substrate concentration was fit to eq 3 (Figure 5C) to provide k_2 and k_3, the latter by subtraction of k_2 from ($k_2 + k_3$). The slower, nearly linear phase of the progress curves (Figure 5A) represents the steady-state rate, v_{ss}, the substrate concentration dependence of which could be fit to the Michaelis−Menten equation (Figure 5D) to provide the steady-state kinetic parameters, K_m and k_{cat}.

These kinetics data are summarized in Table 1. Fitting the data using a concentration of active GH derived from the burst analysis (0.86 μM) is consistent with our observations, whereas using the GH concentration derived from the Bradford assay (3.0 μM) is not. Only when the lower GH concentration was used was k_2 found to be greater than k_3 in fitting eq 3 (Table 1, entry 1 vs 2); the presence of a burst predicts that $k_2 > k_3$. However, when the enzyme concentration was set at 3 μM, as indicated by the Bradford assay,

the calculated k_2 is less than k_3, which is inconsistent with the observation of the burst that is clearly evident in both Figures 4A and 5A. Although several possible explanations for the attenuated burst amplitude are further elaborated in the Discussion, a definitive basis for the observed low values of the burst amplitude is not clear from these data. However, highly reproducible data have been obtained (Figures 4 and 5). By varying substrate concentration at fixed [GH] and fitting equations describing how the burst amplitude and burst rate constant vary with substrate concentration (eq 1−3), we were able to determine the individual rate constants, k_2 and k_3, as well as the dissociation constant, K_s. In so doing, we have learned much about the mechanism of the reaction catalyzed by GH.

Pre-Steady-State Kinetics Experiments for GH and **2**. To determine if the presence of geminal fluorine atoms in **2** changes the rate-limiting step, transient kinetic studies were carried out by rapidly mixing **2** (final concentration 50 μM) with varying concentrations of GH (0.29−1.2 μM). No burst was observed under these conditions (Supporting Information, Figure S3). However, since the substrate concentration was less than K_m (75 μM) and thus nonsaturating, it may be difficult to observe a burst. The experiment was repeated with a higher concentration of **2**, 150 μM.[6] At 150 μM **2**, a modest burst was observed (Figure 6, [GH] = 0.86 μM). The high value of K_m (75 μM) and limited quantity of **2**

Table 1: Burst and Steady-State Kinetics of GH and Abz-Glu-γ-Glu-γ-Tyr(NO₂)

$$E + S \underset{K_S}{\rightleftharpoons} ES \xrightarrow{k_2} ES' \xrightarrow{k_3} E$$
$$\qquad\qquad\quad P_1 \qquad\quad P_2$$

	exponential phase				linear phase	
entry	$K_s\,(\mu M)$	$K_m\,(\mu M)$	$k_2\,(s^{-1})$	$k_3\,(s^{-1})$	$K_m\,(\mu M)$	$k_{cat}\,(s^{-1})$
1[a]	67	2.6	70	83		
2[b]	67	2.6	130	23		
3[c]	67	3.9	75	78	2.6	1.1
4[d]	67	3.9	139	14	2.6	4.0

[a] Fit to the data for the exponential phase (eq 1−3) using Kaleidagraph with the following parameters: [E] = 3 μM (Bradford assay), K_m = 2.60 μM (Figure 5D, Michaelis−Menten equation), $k_2 + k_3$ = 153 s⁻¹ (Figure 5B, eq 2). [b] Fit to the data for the exponential phase (eq 1−3) using Kaleidagraph with the following parameters: [E] = 0.86 μM based on the fraction of active enzyme (28.6%) determined from the ratio of the burst amplitude, A, to [E] (Figure 4); other parameters as in footnote a. [c] Global fit to the data (eqs 1−3) using Dynafit (61) with the following parameter: [E] = 3 μM. [d] Global fit to the data (eqs 1−3) using Dynafit (61) with the following parameter: [E] = 0.86 μM.

available precluded the use of [2] > 150 μM for the collection of data to fit eq 1−3, as was described for substrate **1**. However, fitting the limited data of Figure 6 to the burst equation (eq 1) provided an amplitude of 0.78 μM, or 26% active GH, which is very similar to the value of 29% active GH determined from the kinetic analysis of GH-catalyzed hydrolysis of **1**. At this concentration of substrate, [2] = 150 μM, ∼2K_m, the burst rate constant, k_{burst}, was determined to be 13 s⁻¹.

DISCUSSION

The new continuous fluorescence assay described above provides detailed kinetics data for the hydrolytic reaction catalyzed by γ-glutamyl hydrolase (GH). Previous research to elucidate the kinetic properties of this enzyme has relied on end-point assays (14, 20), primarily via chromatographic separation of the products using high performance liquid chromatography (HPLC) or capillary electrophoresis (CE) (33) (*vide supra*). In order to obtain more detailed steady-state and transient kinetics data, a continuous spectral assay was desired. GH is specific for cleavage of a Glu-γ-Glu bond, releasing glutamic acid, which is neither a fluorophore nor a chromophore. Acylation of the *N*-terminal Glu of the Glu-γ-Glu isopeptide with a fluorescent group together with addition of an internal quenching moiety at the *C*-terminus leads to internal quenching of fluorescence due to FRET (24). GH-catalyzed hydrolysis of these substrates releases the quenching moiety, leading to a fluorescent signal.

The first FRET peptide designed for use as a GH substrate contained an *N*-terminal *p*-(*N*-Me)aminobenzoyl (*N*-Me-*p*-AB) fluorophore with 3-nitrotyrosine (Tyr(NO₂)) as the quenching moiety at the *C*-terminus (23). Although an
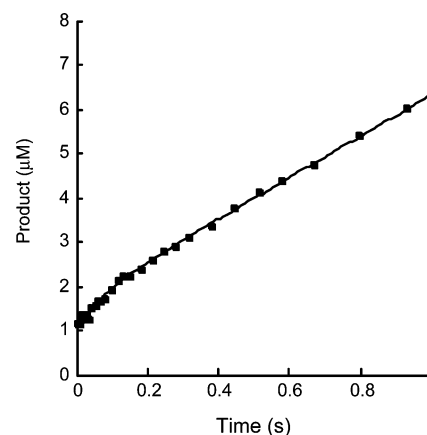
[6] Although the inner filter effect can be a problem at higher substrate concentrations, the stopped-flow instrument was set up to minimize the most severe primary IFE by having the excitation beam pass through the short side of the cuvette (0.75 mm to the center of the cell), and the emission was measured on the long side (5 mm). It should be noted that the IFE will not change the shape of the progress curve, only the amplitude, because absorbance does not change during the course of the reaction.

FIGURE 6: Kinetics of Abz-4,4-F₂Glu-γ-Glu-γ-Tyr(NO₂) (**2**) hydrolysis. Equal volumes of GH in storage buffer (pH 5.5) and **2** in assay buffer (pH 6) were rapidly mixed at 4 °C, and the fluorescence was monitored. Concentrations after mixing were 0.86 μM GH and 150 μM **2**, average traces (*n* = 5) shown.

effective substrate, the hydrolysis of which could be monitored continuously by fluorescence, its utility is limited due to attenuated fluorescence of the reaction products. This is a result of the inner filter effect (IFE) (*vide supra*). Replacement of the *N*-Me-*p*-AB moiety with *o*-aminobenzoyl (Abz) at the *N*-terminus and retention of Tyr(NO₂) at the *C*-terminus minimized the IFE and provided two excellent GH substrates, **1** and its 4,4-difluoroglutamate analogue, **2**, and these have been used to determine the reaction kinetics of GH-catalyzed isopeptide hydrolysis. Product analysis by LC-MS demonstrated that the reaction proceeds with cleavage of the expected Glu-γ-Glu isopeptide bond, leading to Glu-γ-Tyr(NO₂) and Abz-Glu or Abz-(4,4-F₂)Glu from **1** and **2**, respectively (Figure 2). The internally quenched derivatives of Glu-γ-Glu, **1** and **2**, were chosen for study to preclude the possibility of multiple sites of cleavage, as is observed for longer chain poly-γ-glutamates (20, 44). Thus, the kinetics data reported in this paper are for GH-catalyzed hydrolysis of a single bond in a Glu-γ-Glu isopeptide.

While the use of peptide substrates containing fluorophores that are quenched due to intramolecular FRET is common for the high-throughput screening of compound libraries (34, 35), complete evaluation of protease reaction kinetics using such substrates is not frequently found in the biochemical literature (36). This is very likely due to problems caused by quenching of fluorescence (IFE). Recent studies have demonstrated that use of FRET peptides to determine standard enzyme kinetics data (K_m, k_{cat}, k_{cat}/K_m) can lead to incorrect values and erroneous conclusions (37). In such cases, IFE-based errors can be minimized by the use of alternate methods such as fast-flow HPLC (37) or dilution of the fluorogenic peptide substrate with a nonfluorescent analogue (38). In the current research, a proper analysis of the steady-state and kinetics was possible with isopeptide **1** without resorting to these methods (Supporting Information, Figure S2A). However, because the K_m for the fluorinated substrate, **2**, is so large, it was not possible to saturate the enzyme (Supporting Information, Figure S2B) due to the IFE at high concentrations of **2**. The use of fast-flow HPLC was not pursued and the scarcity of (2S)-4,4-difluoroglutamic acid (25) precluded its incorporation into a non-fluorogenic peptide substrate for use in combination with **2**.

A fit of the data shown in Figure S2 (Supporting Information) to the Michaelis−Menten equation provided steady-state kinetic constants for γ-glutamyl peptides **1** and **2** (Table S1). The dramatic decrease in the relative values of k_{cat}/K_m observed rates for GH-catalyzed hydrolysis of **2** vs **1** ($(k_{cat}/K_m)_{rel}$ **2:1** = ca. 0.04) is in contrast to the known inductive effects of fluorine on reactions at adjacent carbon. In the case of regioselective nucleophilic attack at the γ-ester of 4,4-difluoroglutamic acid esters (*25, 39*), the electron-withdrawing properties of fluorine led to a large *increase* in the rate of nucleophilic attack at the adjacent carbon. Interestingly, incorporation of fluorine adjacent to the scissile isopeptide bond results in a significant (~15-fold) increase in K_m. In order to probe more deeply into the basis for the increase in K_m, investigation of GH-catalyzed hydrolysis under non-steady-state conditions was carried out using stopped-flow techniques.

As noted above (eq 4), K_m is composed of a dissociation constant, $K_s = k_{-1}/k_1$, modified by the rates of formation (k_2) and breakdown (k_3) of an intermediate, in this case the acyl enzyme. Experiments to determine the values of K_s, k_2, and k_3 were carried out using the stopped-flow instrument. At a fixed concentration of **1** ([**1**] = ~$10K_m$), GH-catalyzed hydrolysis of the isopeptide displays burst kinetics (Figure 4A), and it can be shown that both the burst amplitude and the steady-state rate are directly proportional to the enzyme concentration (Figure 4B). At a fixed concentration of [GH], hydrolysis of **1** displays burst kinetics (Figure 5A) with the burst rate, k_{burst} (Figure 5B), burst amplitude (Figure 5C) and v_{ss} (Figure 5D) all dependent on the concentration of **1** as predicted. Fitting the data of these figures to eq 2 (Figure 5B), eq 3 (Figure 5C), and the Michaelis−Menten equation (Figure 5D) yielded values of K_s, k_2, k_3, K_m, and k_{cat} (Table 1). The mechanism shown in Figure 3 indicates the reaction steps associated with K_s (k_{-1}/k_1), k_2 and k_3. Intramolecular quenching of fluorescence in **1** is no longer possible on separation of the quenching moiety, Glu-γ-Tyr(NO$_2$), from the fluorescent donor, Abz-Glu, following GH-catalyzed hydrolysis. Since the kinetics of product formation as measured by fluorescence exhibits a rapid burst phase followed by a slower steady-state phase, it follows that the step in which Glu-γ-Tyr(NO$_2$) is released, k_2, must be faster than some subsequent step. As shown in Table 1, the data of Figures 5A−D were fitted in two ways, one of which used the concentration of GH determined by the Bradford assay (3 μM) and a second which used the concentration of GH indicated by the burst amplitude (0.86 μM). Only when [GH] approached 0.86 μM (entries 2 (exponential phase) and 4 (global fit)) were values of k_2 and k_3 obtained that are consistent with the observed burst kinetics; i.e., $k_2 > k_3$. The observation of a burst phase in the enzyme-catalyzed hydrolysis of a peptide bond is unusual. Although the first burst kinetics were reported for a protease (*40*), the substrate used in that classic paper was a nitrophenyl ester. In contrast, substrates **1** and **2** incorporate an isopeptide, Glu-γ-Glu, and, to the best of our knowledge, a pre-steady-state kinetics investigation of enzyme-catalyzed hydrolysis of an isopeptide bond with this structural motif has not been reported (*vide infra*).

It is interesting to note that a more significant burst was observed at 4 °C than at 25 °C (*vide supra*), the temperature at which the steady-state kinetics data (Table S1, Figure S2)

were obtained. Since an increase in fluorescence is associated with release of P$_1$ (Figure 3, k_2), the observed burst at 4 °C suggests, at first glance, that k_2 increases with a decrease in temperature; however, this would be incompatible with the Arrhenius equation, and is therefore unlikely. A more plausible explanation is that k_2 only decreases slightly at the lower temperature while k_3 decreases significantly, so that $k_2 \gg k_3$, leading to the observed burst of fluorescence. The rate constant, k_3, is likely more complex than indicated in Figure 3[5] and could include a product release step and/or protein rearrangement to properly position the active site Cys110 for attack on the adjacent scissile bond if the enzyme acts processively. Large-scale domain motion of GH to accommodate repositioning of the adjacent scissile bond and/or active site residues, included in k_3, would be expected to be much more sensitive to temperature effects than the simple acylation step represented by k_2.

The discrepancy between the apparent concentration of GH as determined by the Bradford assay and that derived from the kinetics data should be addressed. Both the human and rat GH isozymes, the latter expressed and purified as described in the Supporting Information, have been shown to be homogeneous by analytical ultracentrifugation (*41*) and, in the case of human GH, has been crystallized to provide a structure of the substrate-free enzyme (*42*). The simplest explanation of the kinetics data is that only ca. 30% of the enzyme is active.[7] However, there are other possibilities. The X-ray crystal structure of hGH indicated that the enzyme has a homodimer structure with a β-mercaptoethanol molecule covalently linked to Cys110 at only one of the two active sites in the dimer (*42*). In addition, it has been shown recently by analytical ultracentrifugation that GH is a nondissociating homodimer in solution (*20, 41*). Tyr36 is part of the monomer−monomer interface and has shown to be required for catalysis (T.J.R., unpublished results). Thus, it is possible that in hGH, and by extension rGH, only one of the active sites is involved in the burst phase of catalysis; i.e., half-of-the-sites reactivity. The second site burst will be masked by the slower subsequent steps of catalysis. If true, the concentration of GH involved in the burst is predicted to be 50% of the total protein, a figure in closer agreement with the value of ca. 30% determined from the burst amplitude data, but nevertheless suggesting some instability of the protein during handling. It is, of course, also possible that oligomerization to form larger inactive GH aggregates could lead to decreased catalytic activity. However, we have no evidence for the formation of aggregates under the conditions used in the experiments reported herein.

The pre-steady-state kinetics of GH-catalyzed hydrolysis of the 4,4-difluoroglutamate-containing isopeptide, **2**, was

---

[7] More complex kinetics could possibly lead to attenuation of the burst amplitude, including the following: (1) k_2 may have a value similar to k_3; (2) the reverse rate, k_{-2}, may be significant, i.e., a low commitment to catalysis; (3) the rate of substrate binding (k_1[S]) may be similar to k_2; (4) dissociation of the quenching moiety, P$_1$, may be slow and continue to quench the fluorescent acylated enzyme, ES′; or (5) additional species may intervene between ES and ES′, so that some of the enzyme present is not in a form that would be fluorescent. For example, if P$_1$ is released from a species, ES″, that follows ES and is in rapid equilibrium with ES, then the concentration of ES″ will be dependent on the equilibrium constant; e.g., if $K_{eq} = 1$, only 50% of the enzyme could be in the ES″ form that gives rise to the burst. Investigation of these possibilities is beyond the scope of the present study.
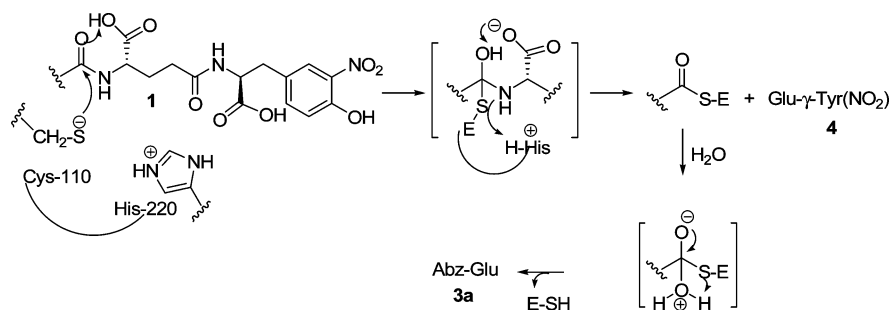
FIGURE 7: Proposed substrate-assisted catalysis in the hydrolysis of Glu-γ-Glu isopeptides.

also investigated using stopped-flow techniques. Due to the IFE, the maximum concentration of **2** used in the acquisition of kinetics data was 150 μM, a concentration of substrate only $\sim 2K_m$. Therefore, a thorough pre-steady-state analysis was not possible. Only when [**2**] = 150 μM ($\sim 2K_m$) was a modest burst observed (Figure 6). The limited data obtained from Figure 6 indicate a >5-fold decrease in k_{burst} for **2** vs **1**, even at subsaturating concentration ($\sim 2K_m$) of the fluorinated substrate. Although modest in magnitude, the effect of placing two fluorine atoms adjacent to the scissile bond in a Glu-γ-Glu isopeptide is to retard the burst phase, presumably associated with formation of the acyl enzyme.[8]

Further analysis of the data presented in Table 1 involving a global fit to the transient kinetics data (Figure 5) allows for evaluation of the internal consistency of these data. Thus, a value of k_{cat} can be calculated from k_2 and k_3 (eq 4), leading to a value of 12.7 s^{-1}, and a value of K_m can be calculated from K_s, k_2, and k_3 (eq 5), leading to a value of 6.1 μM. These calculated values of k_{cat} and K_m for GH-catalyzed hydrolysis of **1** are in reasonable agreement with the steady-state component of the transient kinetics data (Table 1, entry 4).

As noted above, the observation of a burst phase in the GH-catalyzed hydrolysis of **1**, a peptide, albeit an isopeptide, Glu-γ-Glu, is unusual. In terms of substrate structure and site of hydrolysis, the synthetase and hydrolase involved in the reversible post-translational modification of tubulin (*45, 46*) are most closely related to GH. Although the ATP-dependent ligase, tubulin polyglutamylase, that catalyzes the addition of multiple glutamates has been partially purified and its catalytic properties have been described (*47, 48*), the putative hydrolase activity by which the glutamates are removed (*49*) has not been characterized. Other enzymes that catalyze nucleophilic attack at the γ-position of substituted glutamine include γ-glutamyl transpeptidase (EC 2.3.2.2) (*50*) and transglutaminase (EC 2.3.2.13) (*51*). In the former reaction, acylation occurs via attack of an active site Cys or Thr on the γ-carboxamido group of a γ-glutamyl peptide followed by reaction of the acyl enzyme with an amino acid to release the peptide and form a new γ-glutamyl dipeptide. In the latter case, acylation involves attack of an active site cysteine on the γ-carboxamido group of a protein-bound glutamine followed by reaction of the acyl enzyme with an

alkyl amine (e.g., protein-bound lysine, polyamines) to release NH_3 and form a protein-bound γ-substituted glutamine. The catalytic mechanisms of both have been studied in detail but with non-peptide, chromogenic leaving groups (*52*) or nonphysiological amine acceptors (*53, 54*), respectively. Thus, the burst kinetics observed in several cases by these investigators involve substrates with better leaving groups (e.g., *p*-nitroaniline, aminocoumarins) than an amino acid or peptide such as Glu-γ-Tyr(NO₂) released in the GH-catalyzed reaction studied in this work (Figure 5).

Ubiquitin C-terminal hydrolases (UCH) (*55, 56*) are cysteine peptidases, family C12, that act on an isopeptide in which a C-terminal glycine is linked to the ϵ-amino group of an internal lysine residue of ubiquitin (*57*). In extensive mechanistic studies on a ubiquitin C-terminal hydrolase, UCH-L1, Stein and co-workers suggest that the enzyme exhibits a "mechanistic plasticity" where slightly different mechanisms are involved in substrate hydrolysis vs enzyme inactivation by a peptidyl aldehyde (*56*). This suggestion is supported by a crystal structure of apo-UCH-L1 (*58*). It is proposed that binding of the peptide substrate involves displacement of a bound water to allow for proper alignment of the active site His-Cys dyad to form the S$^-$/ImH$^+$ ion pair involved in formation of the acyl enzyme. Similarly, in GH, positioning of Cys110 and His220 to form the requisite ion pair presumably required for GH-catalyzed hydrolysis may involve a significant protein rearrangement, resulting in placing some or all of the substrate in a hydrophobic cleft. Unfortunately, data available from the published crystal structure of hGH (*42*) do not address this possibility because the structure obtained is of the substrate-free enzyme. However, it is possible that GH-catalyzed hydrolysis of oligo-γ-glutamates involves general-acid catalysis by the α-CO₂H of a Glu residue on the carbonyl of the adjacent scissile γ-glutamyl peptide bond. This substrate-assisted catalysis could thereby facilitate attack by Cys110 to form the acyl enzyme intermediate (Figure 7). Substrate-assisted catalysis involving the α-CO₂H could explain the observed decrease in k_{burst} for **2** vs **1**; i.e., electron withdrawal by the CF₂ adjacent to the carbonyl group would render that group less susceptible to general-acid catalysis.

Finally, it should be noted that GH catalyzes the hydrolysis of a polymeric isopeptide and as such may operate in a processive mode as has been demonstrated in glycohydro-lases such as amylase ("degree of multiple attack") (*59*). Although the research reported herein involved a diglutamate substrate containing only a single cleavage site, GH can hydrolyze multiple peptide bonds in longer chain poly-γ-glutamates (*20*). Rearrangement of the initially formed E−P

---

[8] In principle, the rate constant, k_2, which represents the acylation step, could be determined directly via single turnover experiments, which require [E] ≫ [S]. Considering limiting GH solubility at very high concentrations (unpublished data) and the detection limit of ca. 0.2 μM (10% conversion if [S] = 2 μM, $\sim K_m$) for accurate measurement of fluorescence, it proved difficult to design a single turnover experiment that would provide reliable data.

complex to position the next scissile bond for attack by Cys110, as required for a processive mechanism, could be the rate-limiting step. If a rearrangement of E−P slows product release, it could lead to the observed burst kinetics. As noted above, the temperature dependence of k_2 vs k_3, suggested by the observation of a burst of fluorescence at 4 °C but not at 25 °C, is consistent with slow protein rearrangement associated with a processive hydrolytic reaction at sequential peptide bonds along the poly-γ-glutamate chain.

In summary, the hydrolysis of two internally quenched derivatives of the isopeptide, Glu-γ-Glu, by recombinant rat GH has been investigated via a new continuous fluorescence assay. Comparison of the steady-state kinetics data obtained for a substrate with two fluorines adjacent to the scissile bond, **2**, vs the non-fluorinated derivative, **1**, revealed that the surprisingly attenuated rate observed for **2** is due primarily to a 15-fold increase in K_m. Pre-steady-state kinetics data were obtained by stopped-flow fluorescence methods, and a discreet burst phase was observed for the GH-catalyzed hydrolysis of **1**, leading to the conclusion that formation of the putative acyl enzyme occurs with a rate ~10-fold faster than the rate of deacylation and any subsequent step(s). Although the transient kinetics data obtained for **2** were more limited due to the combined effects of a high K_m and the IFE, a modest burst was observed at subsaturating concentrations of the substrate, thus indicating that the two adjacent fluorine atoms do not affect the *relative* rates of formation or breakdown of the acyl enzyme intermediate. This detailed kinetic analysis of GH-catalyzed hydrolysis of **1** has documented an interesting and perhaps unique example of burst kinetics in isopeptide hydrolysis. It has also suggested possible half-the-sites reactivity and a processive mechanism for GH-catalyzed hydrolysis of oligomeric γ-glutamyl substrates, both of which are subjects for future research.

ACKNOWLEDGMENT

SUPPORTING INFORMATION AVAILABLE

Experimental details on the expression and purification of rat GH, synthesis of the GH substrate, *N*-Abz-Glu-γ-Glu-γ-Tyr(NO$_2$) (**1**), by both solution and solid phase methods, two putative products, *N*-Abz-Glu (**3a**) and Glu-γ-Tyr(NO$_2$) (**4**), and a model compound, *N*-Ac-Tyr(NO$_2$) (**S3**), for use in determination of the extinction coefficient of the intact peptide, **1**. Figures showing the linear dependence of product fluorescence on the concentration of the quenched substrate, **1** (Figure S1), steady-state kinetics of the GH-catalyzed hydrolysis of **1** (Figure S2A) and **2** (Figure S2B), and transient kinetics of the GH-catalyzed hydrolysis of **2** at [**2**] $< K_m$ (Figure S3). This material is available free of charge via the Internet at http://pubs.acs.org.

REFERENCES

1. Galivan, J., Ryan, T. J., Chave, K., Rhee, M., Yao, R., and Yin, D. (2000) Glutamyl hydrolase: pharmacological role and enzymatic characterization, *Pharmacol. Ther. 85*, 207−215.
2. Schirch, V., and Strong, W. B. (1989) Interaction of Folylpolyglutamates with Enzymes in One-Carbon Metabolism, *Arch. Biochem. Biophys. 269*, 371−380.
3. Cossins, E. A. (2000) The fascinating world of folate and one-carbon metabolism, *Can. J. Bot. 78*, 691−708.
4. McGuire, J. J., and Coward, J. K. (1984) Folates and Pterins, in *Folates and Pterins* (Blakley, R. L., and Benkovic, S.J., Ed.) pp 135−190, John Wiley and Sons, 1984.
5. Shane, B. (1989) *Vitam. Horm. 45*, 263−335.
6. Chave, K. J., Ryan, T. J., Chmura, S. E., and Galivan, J. (2003) Identification of single nucleotide polymorphisms in the human γ-glutamyl hydrolase gene and characterization of promoter, *Gene 319*, 167−175.
7. Cheng, Q., Wu, B., Kager, L., Panetta, J. C., Zheng, J., Pui, C.-H., Relling, M., and Evans, W. E. (2004) A substrate specific functional polymorphism of human γ-glutamyl hydrolase alters catalytic activity and methotrexate polyglutamate accumulation in acute lymphoblastic leukaemia cells, *Pharmacogenetics 14*, 557−567.
8. Tsukamoto, T., Coward, J. K., and McGuire, J. K. (1996) Fluoroamino Acid Containing Analogues of Folic Acid and Methotrexate, in *Biomedical Frontiers of Fluorine Chemistry* (Ojima, I. M., J. R.; Welch, J. T., Ed.) American Chemical Society, Washington.
9. Licato, N. J., Coward, J. K., Nimec, Z., Galivan, J., Bolanowska, W. E., and McGuire, J. J. (1990) Synthesis of N-[N-(4-Deoxy-4-amino-l0-methylpteroyl)-4-fluoroglutamyl]-γ-glutamate, an Unusual Substrate for Folylpoly-γ-glutamate Synthetase and γ-Glutamyl Hydrolase, *J. Med. Chem. 33*, 1022−1027.
10. Hudlicky, M. (1993) Stereospecific syntheses of all four stereoisomers of 4-fluoroglutamic acid, *J. Fluorine Chem. 60*, 193−210.
11. Tsukamoto, T., Kitazume, T., McGuire, J. J., and Coward, J. K. (1996) Synthesis and biological evaluation of DL-4,4-difluoroglutamic acid and DL-γ,γ-difluoromethotrexate, *J. Med. Chem. 39*, 66−72.
12. Pankuch, J. J. (2004) New Fluorogenic Peptide Substrates for Studying the Mechanism of γ-Glutamyl Hydrolase, Ph.D. Thesis, University of Michigan, Ann Arbor.
13. Uneyama, K. (2006) *Organofluorine Chemistry*, Blackwell Publishing, Oxford, U.K.
14. Wang, Y., Nimec, Z., Ryan, T. J., Dias, J. A., and Galivan, J. (1993) The Properties of the Secreted γ-Glutamyl Hydrolases From H35-Hepatoma Cells, *Biochim. Biophys. Acta 1164*, 227−235.
15. Yao, R. N., Z., Ryan, T. J., and Galivan, J. (1996) Identification, Cloning, and Sequencing of a cDNA Coding for Rat γ-Glutamyl Hydrolase, *J. Biol. Chem. 271*, 8525−8528.
16. Cashmore, A. R., Dreyer, R. N., Horvath, C., Knipe, J. O., Coward, J. K., and Bertino, J. R. (1980) Separation of pteroyl-oligo-γ-L-glutamates by high-performance liquid chromatography, *Methods Enzymol. 66*, 459−468.
17. Jolivet, J., and Schilsky, R. L. (1981) High-Pressure Liquid Chromatography Analysis of Methotrexate Polyglutamates in Cultured Human Breast Cancer Cells, *Biochem. Pharmacol. 30*, 1387−1390.
18. Day, B. P. F., and Gregory, J. F., III (1985) Determination of folylpoly-γ-glutamate carboxypeptidase (folacin conjugase) activity using reversed-phase high-performance liquid chromatography, *J. Chromatogr. 318*, 387−392.
19. Selhub, J. (1989) Determination of Tissue Folate Composition by Affinity Chromatography Followed by High-Pressure Ion Pair Liquid Chromatography, *Anal. Biochem. 182*, 84−93.
20. Orsomando, G., Diaz de la Garza, R., Green, B. J., Peng, M., Rea, P. A., Ryan, T. J., Gregory, J. F., III, and Hanson, A. D. (2005) Plant γ-Glutamyl Hydrolases and Folate Polyglutamates: Characterization, Compartmentation, and Co-Occurrence in Vacuoles, *J. Biol. Chem. 280*, 28877−28884.
21. Waltham, M. C., Li, W. W., Gritsman, H., Tong, W. P., and Bertino, J. R. (1997) γ-Glutamyl hydrolase from human sarcoma

HT-1080 cells: Characterization and inhibition by glutamine antagonists, *Mol. Pharmacol. 51*, 825−832.

22. Rhee, M. S., Lindau-Shepard, B., Chave, K. J., Galivan, J., and Ryan, T. J. (1998) Characterization of human cellular γ-glutamyl hydrolase, *Mol. Pharm. 53*, 1040−1046.

23. Pankuch, J. J., and Coward, J. K. (2001) *N*-Me-*p*AB-Glu-γ−Glu-γ-Tyr(3-NO₂): An Internally Quenched Fluorogenic γ-Glutamyl Hydrolase Substrate, *Bioorg. Med. Chem. Lett. 11*, 1561−1564.

24. Lakowicz, J. R. (1999) *Principles of Fluorescence Spectroscopy*, Kluwer Academic/Plenum Publishers, New York.

25. Konas, D. W., Pankuch, J. J., and Coward, J. K. (2002) The Synthesis of (2S)-4,4-Difluoroglutamyl γ-Peptides Based on Garner's Aldehyde and Fluoro-Reformatsky Chemistry, *Synthesis 17*, 2616−2626.

26. Bradford, M. M. (1976) A Rapid and Sensitive Method for the Quantitation of Microgram Quantities of Protein Utilizing the Principle of Protein-Dye Binding, *Anal. Biochem. 72*, 248−254.

27. Bender, M. L., Kezdy, F. J., and Wedler, F. C. (1967) α-Chymotrypsin: Enzyme Concentration and Kinetics, *J. Chem. Educ. 44*, 84−88.

28. Johnson, K. (1992) Transient State Kinetic Analysis of Enzyme Reaction Pathways, in *Mechanisms of Catalysis* (Sigman, D. S., Ed.) 3rd ed., pp 1−61, Academic Press, Inc., San Diego.

29. Fu, S. C. J. (1965) A New Synthesis of *p*-Methylaminobenzoyl-L-Glutamic Acid, *J. Org. Chem. 30*, 1277.

30. Chakraborty, D. P., Roy, S., Chakraborty, A. K., and Rakshit, R. (1989) Tryptophan Participation in Melanogenesis−Modification of Raper-Mason-Pawelek Scheme of Melanin Formation, *J. Indian Chem. Soc. 66*, 699−702.

31. Silverman, R. B. (2002) *The Organic Chemistry of Enzyme-Catalyzed Reactions*, Academic Press, San Diego.

32. Skarzynski, T. K., D. H., Lees, W. J., Walsh, C. T., and Duncan, K. (1998) Stereochemical Course of Enzymatic Enolpyruvyl Transfer and Catalytic Conformation of the Active Site Revealed by the Crystal Structure of the Fluorinated Analogue of the Reaction Intermediate Bound to the Active Site of the C115A Mutant of MurA, *Biochemistry 37*, 2572−2577.

33. Chave, K. J., Galivan, J., and Ryan, T. J. (2003) γ-Glutamyl hydrolase, (Woessner, F., Rawlings, N., and Barrett, A., Eds.) 2nd ed., pp 1396−1399, Academic Press, New York.

34. Meldal, M. (2002) The one-bead two-compound assay for solid phase screening of combinatorial libraries, *Biopolymers 66*, 93−100.

35. Goddard, J. P., and Reymond, J. L. (2004) Recent advances in enzyme assays, *Trends Biotechnol. 22*, 363−370.

36. Stein, R. L., Barbosa, M. D. F. S., and Bruckner, R. (2000) Kinetic and mechanistic studies of signal peptidase I from Escherichia coli, *Biochemistry 39*, 7973−7983.

37. Kruger, R. G. D., P., and McCafferty, D. G. (2004) Development of a high-performance liquid chromatography assay and revision of kinetic parameters for the Staphlococcus aureus sortase transpeptidase SrtA, *Anal. Biochem. 326*, 42−48.

38. Thomas-Wohler, J., and Lee, I. (2002) Kinetic characterization of the peptidase activity of Escherichia coli Lon reveals the mechanistic similarities of ATP-dependent hydrolysis of peptide and protein substrates, *Biochemistry 41*, 9418−9425.

39. Tsukamoto, T., and Coward, J. K. (1996) Facile synthesis of DL-4,4-difluoroornithine, DL-4,4-difluoroglutamine, and γ-DL-4,4-difluoroglutamyl-containing peptides: regiospecific addition of nucleophiles to *N*-Cbz-di-*tert*-butyl-DL-4,4-difluoroglutamate, *J. Org. Chem. 61*, 2497−2500.

40. Hartley, B. S., and Kilby, B. A. (1954) The reaction of *p*-nitrophenyl esters with chymotrypsin and insulin, *Biochem. J. 56*, 288−297.

41. Eisele, L. E., Chave, K. J., Lehning, A. C., and Ryan, T. J. (2006) Characterization of human γ-glutamyl hydrolase in solution demonstrates that the enzyme is a non-dissociating homodimer, *Biochem. Biophys. Acta 1764*, 1479−1486.

42. Li, H. M., Ryan, T. J., Chave, K. J., and Van Roey, P. (2002) Three-dimensional structure of human γ-glutamyl hydrolase: A class I glutamine amidotransferase adapted for a complex substrate, *J. Biol. Chem. 277*, 24522−24529.

43. Chave, K. J., Auger, I. E., Galivan, J., and Ryan, T. J. (2000) Molecular Modeling and Site-directed Mutagenesis Define the Catalytic Motif in Human γ-Glutamyl Hydrolase, *J. Biol. Chem. 275*, 40365−40370.

44. Silink, M., Reddel, R., Bethel, M., and Rowe, P. B. (1975) γ-Glutamyl Hydrolase (Conjugase), *J. Biol. Chem. 250*, 5982−5994.

45. MacRae, T. H. (1997) Tubulin post-translational modifications - Enzymes and their mechanisms of action, *European J. Biochem. 244*, 265−278.

46. Westermann, S., and Weber, K. (2003) Post-translational modifications regulate microtubule function, *Nat. Rev. Mol. Cell Biol. 4*, 938−947.

47. Regnard, C., Audebert, S., Desbruyeres, E., Denoulet, P., and Edde, B. (1998) Tubulin polyglutamylase: Partial purification and enzymatic properties, *Biochemistry 37*, 8395−8404.

48. Westermann, S., and Weber, K. (2002) Identification of CfNek, a novel member of the NIMA family of cell cycle regulators, as a polypeptide copurifying with tubulin polyglutamylation activity in *Crithidia*, *J. Cell. Sci. 115*, 5003−5012.

49. Audebert, S., Desbruyeres, E., Gruszczynski, C., Koulakoff, A., Gros, F., Denoulet, P., and Edde, B. (1993) Reversible polyglutamylation of α- and β-tubulin and microtubule dynamics in mouse-brain neurons, *Mol. Biol. Cell 4*, 615−626.

50. Keillor, J. W., Castonguay, R., and Lherbet, C. (2005) γ-glutamyl transpeptidase substrate specificity and catalytic mechanism, *Methods Enzymol. 401*, 449−467.

51. Folk, J. E., and Chung, S. I. (1985) Transglutaminases, *Methods Enzymol. 113*, 358−375.

52. Keillor, J. W., Menard, A., Castonguay, R., Lherbet, C., and Rivard, C. (2004) Pre-steady-state kinetic studies of rat kidney γ-glutamyl transpeptidase confirm its ping-pong mechanism, *J. Phys. Org. Chem. 17*, 529−536.

53. Case, A., and Stein, R. L. (2003) Kinetic Analysis of the Action of Tissue Transglutaminase on Peptide and Protein Substrates, *Biochemistry 42*, 9466−9481.

54. Chica, R. A., Gagnon, P., Keillor, J. W., and Pelletier, J. N. (2004) Tissue transglutaminase acylation: Proposed role of conserved active site Tyr and Trp residues revealed by molecular modeling of peptide substrate binding, *Protein Sci. 13*, 979−991.

55. Dang, L. C., Melandri, F. D., and Stein, R. L. (1998) Kinetic and mechanistic studies on the hydrolysis of ubiquitin C-terminal 7-amido-4-methylcoumarin by deubiquitinating enzymes, *Biochemistry 37*, 1868−1879.

56. Case, A., and Stein, R. L. (2006) Mechanistic studies of ubiquitin C-terminal hydrolase L1, *Biochemistry 45*, 2443−2452.

57. Wilkinson, K. D. (2000) Ubiquitination and deubiquitination: Targeting of proteins for degradation by the proteasome, *Cell Dev. Biol. 11*, 141−148.

58. Das, C., Hoang, Q. Q., Kreinbring, C. A., Luchansky, S. J., Meray, R. K., Ray, S. S., Lansbury, P. T., Ringe, D., and Petsko, G. A. (2006) Structural basis for conformational plasticity of the Parkinson's disease-associated ubiquitin hydrolase UCH-L1, *Proc. Natl. Acad. Sci. U.S.A. 103*, 4675−4680.

59. Kramhoft, B., Bak-Jensen, K. S., Mori, H., Juge, N., Nohr, J., and Svensson, B. (2005) Involvement of individual subsites and secondary substrate binding sites in multiple attack on amylose by barley α-amylase *Biochemistry 44*, 1824−1832.

60. Riordan, J. F., Sokolovsky, M., and Vallee, B. L. (1967) Environmentally Sensitive Tyrosyl Residues. Nitration with Tetranitromethane, *Biochemistry 6*, 358−361.

61. Kuzmic, P. (1996) Program DYNAFIT for the Analysis of Enzyme Kinetic Data: Application to HIV Proteinase, *Anal. Biochem. 237*, 260−273.